APPLICATION MODELLING OF INTELLIGENT DIAGNOSIS FOR THERMAL CYCLE SYSTEM

by

Chunda LIANG *

Tourism College of Changchun University, Changchun, China

Original scientific paper
https://doi.org/10.2298/TSCI2302101L

In order to solve the problem of intelligent fault diagnosis of thermal system of thermal power unit, the application modelling of intelligent diagnosis of thermal cycle system is proposed. This paper first filters the influence of the change of valve opening of steam turbine on the performance index under the condition of constant power, and qualitatively analyzes the actual change of the performance index compared with the reference working condition when the component fails, so as to eliminate the mutual influence between the components. Then, the selection principle of thermodynamic parameters is determined, the irreversible loss in the structural theory of thermal economics is introduced as the performance index, and the model is used to quantitatively calculate the change of performance index of each component under fault conditions to diagnose the failed component. Finally, APROS simulation software is used to simulate various fault conditions of 330 MW units in a power plant. The experimental results show that the recognition accuracy of the monitoring system designed in this paper can reach 98.33%. In conclusion, the method in this paper proves the feasibility of intelligent fault diagnosis of thermodynamic system network.

Key words: *fault diagnosis, characteristic curve, performance index, deep learning, machine vision technology*

Introduction

With the continuous development of the power industry, more and more large units have been put into operation of the power plant, and the capacity of the main units has increased (300 MW, 600 MW). Once the unit downtime, in addition the power plant itself caused huge economic losses, will also have a great impact on the entire power grid, causing significant economic losses and social consequences. In order to ensure the safe and reliable operation of the system, it is necessary to study the fault diagnosis of power plant production, in order to find the fault as early as possible, deal with it in time, and reduce the loss to the minimum. Thermal system is the main part of power plant production, this part of the fault diagnosis is particularly important.

With the continuous development of intelligent technology, the research on fault diagnosis technology of thermal power plant will be further developed to the measurement point optimization, fault location, multi-fault diagnosis, fault prediction and fault diagnosis system integration. This process will be closely integrated with the lifetime diagnosis of equipment, intelligent technology (especially knowledge acquisition and control between knowledge levels) and information fusion technology, at the same time, the role of domain knowledge and domain experts will become more important. As shown in fig. 1.

* Author's e-mail: ChundaLiang@163.com

Figure 1. Machine vision technology

Literature review

Deep learning is one of the key research directions of machine learning, by learning the internal rules and representation levels of a large number of samples, data analysis ability like human brain can be formed, its performance in the field of image information recognition and image information fusion has been widely recognized. In order to this end, the author combined the deep learning algorithm with machine vision technology, and based on the deep learning algorithm, sensed multiple vision sensors to collect the network fault data of the thermal system [1]. Machine vision systems based on deep learning can be complementary to traditional machine vision. In order to ensure the safety and stability of power plant operation, scholars at home and abroad have done a lot of research on this problem, and developed a variety of diagnostic methods for power plant thermal system or some equipment fault diagnosis, and achieved certain results. Wang *et al*. [2] adopted two mathematical criteria obtained through thermal economic analysis to identify components where faults occur. Wang *et al*. [3] obtained the fault data by establishing the thermodynamic simulation model, and introduced the thermal economic structural theory diagnosis model to complete the fault source location. Zhao *et al*. [4] proposed an intelligent diagnosis method, which applied fuzzy neural network (FNN) for local diagnosis, multi-source information fusion technology is used for global diagnosis, which can quickly and accurately complete the task of single fault diagnosis and multiple fault diagnosis of different types. Foreign scholars have continuously improved and applied the structural theory of thermal economics based on analytical methods, Miri *et al*. [5]. This paper studies the additional resource consumption caused by the intervention of the control system, and takes the lead in proposing the influence caused by the control system in the process of filtering diagnosis.

Methods

Establishment of the model

In the thermal system of a thermal power plant, each component has a corresponding index to evaluate its operating performance, and this index has a certain functional relationship with the thermal parameters of the component. Therefore, it can be considered that each component in the system has a thermal parameter – performance index characteristic curve, this curve indicates that there exists a series of relations f so that the performance index, κ, of components is a function of a set of thermodynamic parameters τ:

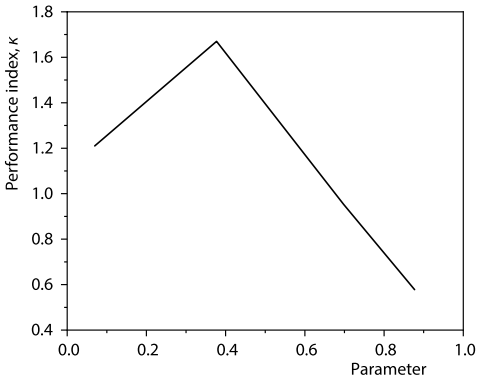

Figure 2. Schematic diagram of thermodynamic parameter – performance index characteristic curve

$$\kappa = f(\tau) \tag{1}$$

For any component, the characteristic curve of the corresponding performance index of a certain thermodynamic parameter under the reference and fault conditions can be obtained by assumption, their functional relations are f_{wi} and f_{mal}, as shown in fig. 2. Once the working condition is determined, this functional relation will

be determined accordingly. Therefore, it can be considered that the characteristic curve of the reference working condition is invariant under certain boundary conditions of the system, and the characteristic curve will change only when the component fails [6].

Under the premise of maintaining the same shaft power as the reference working condition, the thermal parameters of each component in the fault working condition will change. As shown in fig. 1, if there is A fault in a part, when its thermal parameters change from τ_1 to τ_2, the operating performance point of the part will change from the reference state A to a new state C. The difference in value between two state said the change of the component performance $\Delta\iota$ also said so quantitative:

$$\Delta\iota = f_{\text{mal}}(\tau_2) - f_{\text{ref}}(\tau_1) \tag{2}$$

If there is no fault in the component and only the reference working condition characteristic curve is considered, then when the thermodynamic parameter produces $\Delta\tau$ change, the operating performance point of the component will change from state A to state D, indicating that the component will also produce the change of performance index $\Delta\delta$ under trouble-free working condition:

$$\Delta\delta = f_{\text{ref}}(\tau_2) - f_{\text{ref}}(\tau_1) \tag{3}$$

In fact, the process of going from point A to point C can be broken down into going from point A to point D and then to point C. Therefore, the actual fault $\Delta\gamma$ (CD section) of components under fault conditions should be the total performance change $\Delta\iota$ (CF section), minus the performance index change $\Delta\delta$ (DF section) that will occur only with the thermal parameter change of components without fault:

$$\Delta\gamma = f_{\text{mal}}(\tau_2) - f_{\text{ref}}(\tau_2) = \Delta\iota - \Delta\delta \tag{4}$$

where $\Delta\gamma$ only represents the performance change caused by the fault of the component itself, theoretically, the influence of other components on it is eliminated (that is, the induced fault), and the mutual influence between components is decoupled [7].

Eliminate the influence of valve opening on performance indicators

Since the unit is usually connected to the grid in practice, its output power is often required to reach a certain value. Therefore, it is more practical to discuss the model under the condition of constant power than constant flow.

Under the fault condition of keeping the power constant, the flow will increase. Adjust the system action, the valve opening changes will cause additional impact on the system performance indicators, accurate identification of interference diagnosis source. Some scholars have proposed a method to eliminate the influence caused by the regulation system, the basic idea is to imagine a faulty component condition with both the valve opening and the faulty condition of the reference condition. The author puts forward a new imaginary working condition point and compares it with the fault condition eliminate the influence of valve.

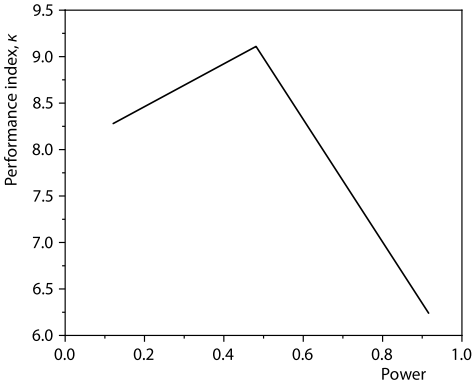

Figure 3. Schematic diagram of the effect of valve opening on performance index

It is assumed that the power-performance index characteristic curves of any component under reference and fault conditions have been obtained, as shown in fig. 3.

Qualitative analysis of actual variation of performance indicators

According to the previous analysis, in order to eliminate the additional influence of the regulation system action, Point B of state is used instead of Point A as the reference benchmark. In order to this end, $\Delta\delta$ in fig. 1 is deducted from the difference $\Delta\rho$ between the performance indexes of two reference Points A and B, and a new index $\Delta\pi$ is obtained:

$$\Delta\pi = f_{\text{ref}}(\tau_2) - f_{\text{ref}}(\tau_3) = \Delta\delta - \Delta\rho \tag{5}$$

where $\Delta\pi$ is the performance index change of components with the change of thermodynamic parameters when point B is taken as the benchmark under free working condition. Equation (4) can also be re-written:

$$\Delta\gamma = \Delta\iota - \Delta\rho - \Delta\pi \tag{6}$$

Due to two filters on valve opening effects and component interactions, $\Delta\gamma$ is the actual change of the component performance index. Therefore, in the case of obtaining a component characteristic curve, $\Delta\rho$ and $\Delta\pi$ can be used to calculate $\Delta\gamma$, so as to diagnose the fault of the component:

$$\Delta\pi = f_{\text{ref}}(\tau_2) - f_{\text{ref}}(\tau_3) \approx \sum_k \left(\frac{\partial f_{\text{ref}}}{\partial \tau_k}\right)_{\tau_3} (\tau_2 - \tau_3) = \Delta\zeta \tag{7}$$

where n partial derivatives can be solved by simultaneous n of the following equations, which is the approximate value of the partial derivative term in eqs. (8) and (9):

$$\Delta\tau_k, n\left(\frac{\partial f_{\text{ref}}}{\partial \tau_k}\right)_{\tau_3} \approx \Delta\pi_n \tag{8}$$

where n represents the number of a series of trouble-free working conditions near the free working condition point, and its value is equal to τ_k:

$$\Delta\kappa = \Delta\iota - \Delta\rho - \Delta\zeta = \Delta\iota - \Delta\rho - \sum_k \left(\frac{\partial f_{\text{ref}}}{\partial \tau_k}\right)_{\tau_3} \Delta\tau_k \tag{9}$$

Deep learning visual inspection system

Overall structure of deep learning visual inspection system

On the left is the offline part: after collecting positive and negative sample pictures in the field, and taking them as input, the adaptive neural network model is calculated by Python's deep learning library, and the model is imported at runtime for error-proof calculation.

On the right is the field runtime detection system software, which contains the following modules: the image acquisition module of the camera, the communication module for communicating with PLC, the deep learning algorithm module, the database recording module, the parameter setting module and the interface UI. When realizing the corresponding functions, UI calls each function module to realize the complete functions of picture acquisition, picture processing, result recording, parameter setting and result return. The PLC communication module based on SNAP7 protocol first detects the picture acquisition trigger signal given by PLC in real time, and the collected picture is preprocessed, such as clipping and homogenization, and then transmitted to the deep learning algorithm module, which calculates the error prevention result. The error prevention result is written into the DB block of PLC through the PLC communication module, and the result is recorded to the local database at the same time [8].

Selection of hardware used in deep learning visual inspection system

The hardware of vision system mainly includes camera, lens and light source.

The selection of camera is mainly based on the detection accuracy and field of view of the vision system. The selection of lens mainly considers the detection environment. The selection of light source is based on making the important features of the measured object appear, and as far as possible to avoid the negative impact of ambient light.

As shown in tab. 1, the camera type selected by this detection system is an ordinary industrial camera, the detection accuracy is required to be 1 mm, and the field of view is 600 mm × 200 mm, according to the resolution F = field of view/detection accuracy, it can be known that the camera resolution is at least 600, considering the resolution parameters and cost of most cameras on the market, it is confirmed that 130 W (1280 × 1024) pixel industrial camera is selected, and the product model is acA1300 – 30gc. According to the sensor size of the camera and the lay-out of the site, the working distance of the vision system is 500 mm, according to the focal length of the lens f = object distance × sensor size/field of view, the wide-angle lens with a focal length of 4 mm is selected. According to the detection needs of this case and based on the robustness brought by deep learning, ordinary LED infrared strip light source can be used to meet the detection needs, and the light source model is LIM – 800 × 40 – IR –W_0.

Table 1. Hardware parameters of the vision system

Camera model	Image sensor size	Field of view	Resolution	Wavelength	Type description	Lens	Light type
acA1280 – 60gc	1280 × 1024	600 mm × 200 mm	2.1 pixels/ mm	Infrared, 850 nm	Infrared bar light	4 mm extension ring	LIM – 400 × 40 – IR – W

Experimental analysis

The model is applied to the performance diagnosis of a 330 MW thermal power unit. The model of the steam turbine unit is N330-16.67/538/538, the flow through part is composed of one high pressure cylinder, one medium pressure cylinder, two low pressure cylinders, one condenser, and one small steam engine, the regenerative system consists of three high pressure heaters, one deaerator, four low pressure heaters, one hydrophobic cooler, one shaft seal heater, one feed pump, and one condensate pump. The first heater is the heater with the highest extraction pressure, and so on, seventh heater is the heater with the lowest extraction pressure, and each heater is connected by hydrophobic self-flow step by step.

The established APROS model was used to simulate three fault conditions under the reference condition and the constant power condition, the fault-free condition with the same valve opening as the fault condition (*i.e.*, the free condition point), and the fault-free condition near several free condition points, the thermal parameters of each component under different working conditions are obtained. The heat consumption guarantee condition (THA) without fault is selected by reference to the operating condition. The fault-free condition near the free condition point is obtained by adjusting the main steam flow. The three fault conditions include:

– The efficiency of the first stage of the regulating stage and the middle pressure cylinder decreases by 5%.
– The second high plugging pipe 10% and fault condition 1 occur at the same time.
– Under 80% variable working conditions, the efficiency of the first stage of the regulating stage and the high pressure cylinder decreases by 5%, and the third high blocking pipe decreases by 10%.

Because these three working conditions simulate the common faults in the actual operation of the unit, and consider the failure under variable working conditions, the diagnosis results are representative to a certain extent.

Taking fault Condition 1 as an example, the unit was divided into several parts to be diagnosed, and the thermal parameters simulated by APROS were used to calculate the exergic flow per share in fig. 3 under different conditions, and according to the irreversible loss of each component under reference condition, fault condition and free condition. Then $\Delta\iota$ in eq. (10) can be re-written:

$$\Delta\iota_{C\to f} = I_{C-i,\text{mal}} - I_{C-,\text{ref}} \tag{10}$$

where $\Delta\rho$ in eq. (5) is:

$$\Delta\rho_{C-s} = I_{C-s,\text{free}} - I_{C\to,\text{ref}} \tag{11}$$

Results and discussion

In the calculation, the thermodynamic parameters of other stages of the turbine are selected the same as those of the regulating stage. The thermal parameters of the heater are inlet water pressure, inlet water temperature, outlet water pressure, outlet water temperature and extraction flow rate. Superheater and reheater choose outlet steam pressure, steam flow rate and inlet working medium pressure. All kinds of pumps choose inlet working medium pressure, temperature and flow. The steam inlet pressure, steam inlet enthalpy, condensate pressure and flow rate are selected for the condenser. The number of fault-free operating conditions simulated near the free operating point should be equal to the thermal parameters selected for each component. In addition, since fault Condition 3 occurs under variable working conditions, the corresponding reference condition is selected as the 80% heat consumption guarantee condition, and the power is also kept at 80% rated power [9, 10].

The 100 pictures of the thermal system were used in the test (including 50 pictures of the normal thermal system and 50 pictures with fault conditions) for three tests. Firstly, the image segmentation algorithm proposed by the author is used for preprocessing, and then the convolutional neural network is used to classify and recognize the preprocessed images. The processing results obtained are shown in tab. 2.

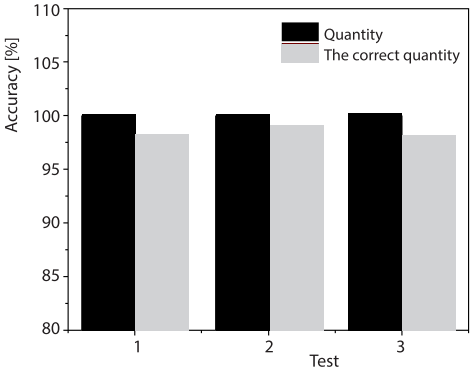

Figure 4. Comparative analysis of image recognition

Table 2. Image recognition results

Test	Number	Right amount	Correct
1	100	98	98%
2	100	99	99%
3	100	98	98%

According to tab. 2 and fig. 4, the recognition accuracy of the monitoring system designed by the author can reach 98.33%.

In order to present the methods and ideas proposed more clearly and visually, taking the regulation stage as an example, the calculation results of the regulation stage under three fault conditions are expressed quantitatively. Taking fault Condition 3 as an example, Point A is the reference condition point where no fault occurs,

when the unit power is kept constant, the state Point C under fault condition can be obtained. However, the AC segment cannot represent the real index change caused by the efficiency decline of the regulator stage, therefore, Point D, which has the same boundary conditions as Point C under the reference working condition, should also be considered, the difference between AC segment and AD segment is the actual index change caused by the failure of the regulator stage. In the case of constant power, the change of regulating valve opening will cause interference to the performance index, so it is necessary to filter the influence of regulating stage, thus, the free working condition Point B is introduced, namely, the imaginary fault-free working condition point with the same valve opening as the working condition Point C. It can be seen from the calculation results that the power of Point B increases and the performance index changes compared with Point A. Taking Point B instead of point A as the reference, the index change affected by valve opening is eliminated, which is the process of BCD.

Through the aforementioned quantitative analysis, the following conclusions can be drawn:

– Under the three fault conditions, each faulty part will affect other non-faulty parts, resulting in induced faults. As shown in tab. 1, in fault Condition 1, due to the failure of the regulating stage, the exhaust enthalpy of the high pressure cylinder increases and the heat absorption of the reheater decreases, so the irreversible loss is negative. At the same time, the increase of exhaust enthalpy of high pressure cylinder will lead to insufficient output of high pressure cylinder, in order to ensure certain output, it is necessary to increase the flow rate, so that the heat absorption in the boiler increases, so the irreversible loss is positive. The failure of Level 1 group of medium pressure cylinder finally causes the increase of exhaust enthalpy of low pressure cylinder, the condenser cold source loss increases, so a large irreversible loss is generated, and its negative value is due to the negative entropy in the system containing the condenser. In fault Condition 2, the increase of end difference of second high additive will cause a large irreversible loss of first high additive. Similarly, under fault Condition 3, the fault of third Gaoga will also affect second Gaoga. The decrease of the efficiency of the regulator stage and the first stage group of the high pressure cylinder will affect the exhaust enthalpy of each cylinder, so as to affect the heat absorption of the boiler, reheater and condenser, and cause a great change of irreversible loss.
– By introducing $\Delta\rho$ and $\Delta\zeta$, the variation of performance index is filtered twice, basically, the fault induced by the faulty component on the non-faulty component can be eliminated, that is, the $\Delta\kappa$ of the non-faulty component should be 0. Although the $\Delta\kappa$ value of non-faulty parts is obviously smaller than that of faulty parts, it does not change to 0. This can be understood as an error ε.

Conclusion

The author proposes the application of machine vision technology and deep learning in network fault diagnosis of thermal system, the overall functional structure of intelligent fault diagnosis system of thermal system of thermal power unit, according to the main algorithm module of the model software, the fuzzy mathematical expression methods of semantic type and trend type are discussed in detail in fault diagnosis of power station thermal system, the comprehensive application can effectively increase the timeliness of the fault diagnosis process and the stability and reliability of the diagnosis results. Two intelligent fault diagnosis models, fuzzy pattern recognition and ANN, are presented, and the technical points of the two models are discussed. These technologies have been used in the development of an intelligent fault diagnosis system for thermal power units, and good results have been achieved.

Reference

[1] Jung, Y., Cho, M. K., Impacts of Reporting Lines and Joint Reviews on Internal Audit Effectiveness, *Managerial Auditing Journal*, *37* (2022), 4, pp. 486-518
[2] Wang, R., *et al.*, Cultivating Consumer Subjective Well-Being through Online Brand Communities: A Multidimensional View of Social Capital, *Journal of Product and Brand Managemen*t, *31* (2022), 5, pp. 808-822
[3] Wang, Q., Wei, S., Development and Application of Methane Leakage Monitoring System for Gas Transmission Pipe-Line, *Electronic Research and Application*s, *5* (2021), 6, pp. 44-49
[4] Zhao, Y., *et al*., Modelling and Dynamics Simulation of Spur Gear System Incorporating the Effect of Lubrication Condition and Input Shaft Crack, *Engineering Computations*, *39* (2022), 5, pp. 1669-1700
[5] Miri, S., *et a*l., Tensile and Thermal Properties of Low-melt Poly Aryl Ether Ketone Reinforced with Continuous Carbon Fiber Manufactured by Robotic 3-D Printing, *The International Journal of Advanced Manufacturing Technology*, *122* (2022), 2, pp. 1041-1053
[6] Hegde, N., *et al*., A Survey on Machine Learning and Deep Learning-Based Computer-Aided Methods for Detection of Polyps in CT Colonography, *Current Medical Imaging Reviews*, *17* (2021), 1, pp. 3-15
[7] Parham, Kebria, M., *et al.*, Deep Imitation Learning for Autonomous Vehicles Based on Convolutional Neural Networks, *IEEE/CAA Journal of Automatica Sinica*, *7* (2020), 01, pp. 85-98
[8] Ghosh, M. K., Pradhan, S., A Non-Zero-Sum Risk-Sensitive Stochastic Differential Game in the Orthant, *Mathematical Control, Related Fields*, *12* (2022), 2, pp. 343-370
[9] Alkheder, S., *et al*., A Socio-Economic Study for Establishing an Environment-Friendly Metro in Kuwait, *International Journal of Social Economic*s, *49* (2022), 5, pp. 685-709
[10] Cai, W., Hu, D., The Qrs Complex Detection Using Novel Deep Learning Neural Networks, *IEEE Access*, *8* (2020), May, pp. 97082-97089

Paper submitted: July 18, 2022
Paper revised: September 7, 2022
Paper accepted: September 22, 2022